Phase Space Stability Error Control with Variable Time-stepping Runge- Kutta Methods for Dynamical Systems *

Tony Humphries **1 and **R.Vigneswaran** ***2

1 Room 1116, Burnside Hall, Department of Mathematics and Statistics, McGill University, 805 Sherbrooke West, Montreal, Quebec H3A 2K6, Canada.

2 Department of Mathematics and Statistics, University of Jaffna, Thirulnelvely(N.P), Sri Lanka

We consider a phase space stability error control for numerical simulation of dynamical systems. We illustrate how variable time-stepping algorithms perform poorly for long time computations which pass close to a fixed point. A new error control was introduced in [9], which is a generalization of the error control first proposed in [8]. In this error control, the local truncation error at each step is bounded by a fraction of the solution arc length over the corresponding time interval. We show how this error control can be thought of either a phase space or a stability error control. For linear systems with a stable hyperbolic fixed point, this error control gives a numerical solution which is forced to converge to the fixed point. In particular, we analyze the forward Euler method applied to the linear system whose coefficient matrix has real and negative eigenvalues . We also consider the dynamics in the neighborhood of saddle points. We introduce a step-size selection scheme which allows this error control to be incorporated within the standard adaptive algorithm as an extra constraint at negligible extra computational cost. Theoretical and numerical results are presented to illustrate the behavior of this error control.

1 Introduction

Variable time-stepping algorithms are often used to solve the dynamical systems defined by autonomous initial value ordinary differential equations (ODEs)

$$y_t = f(y), \qquad y(0) = y^0 \in \mathbb{R}^m, \tag{1}$$

where $f : \mathbb{R}^m \to \mathbb{R}^m$ is assumed to be Lipschitz continuous.

In a dynamical systems context an accurate solution of (1) over a given finite time-interval with a particular y^0 is often of little relevance; rather, it is the global behavior of the system for general values of y^0 in the limit as $t \to \infty$ that is of interest.

When a fixed time-stepping numerical method is used to approximate the flow of (1) on or near to a chaotic attractor the error between the numerical approximation and exact solution grows exponentially in time. This leads us to question the meaningfulness of the numerical solution in the limit as $t \to \infty$. This issue has now been studied in detail, and the approach of considering the numerical solution as a discrete dynamical system in its own right, and then comparing the dynamics of this system with the dynamics of (1), has been particularly fruitful (see [12] and the references therein).

It is widely accepted that to be efficient an ODE algorithm must be adaptive; that is, the step-size must be varied according to some error measure. In contrast to the fixed step-size case, a dynamical systems oriented theory for variable step-size algorithms is far from complete. Contributions in this area include [2, 5, 6] on

---

behavior near stable equilibria, [7, 11] on systems with particular nonlinear structures, and [1] on spurious fixed points.

Although typical adaptive algorithm performs well during finite time integration with fixed initial condition,it is observed that three areas in which this algorithm performs badly. The first is behavior around a stable fixed point. Hall [5] showed that typical methods fail to capture the correct dynamics in this very simple and important scenario. An illustration of this behavior was given in [8]. A second area where poor behavior can arise was identified in [1], where it was shown that almost all adaptive explicit Runge-Kutta methods admit stable *spurious* fixed points for arbitrarily small tolerances.

The third area of poor performance of a typical adaptive ODE algorithm, and perhaps the most important in a dynamical systems context, is near to saddle points. In a chaotic attractor it is often the unstable manifolds of the fixed points which organdie the flow on the attractor. The numerical solution will thus only be give a good approximation to the flow on the attractor if it models the unstable manifolds well. But to do this it must produce good approximations to the local unstable manifolds. It was shown in [8], and is illustrated again in section 4.2 that the typical adaptive ODE algorithm fails to do this. Trajectories of (1) which approach a saddle point close to the stable manifold and should pass close to the fixed point before exiting close to the unstable manifold, can result in numerical trajectories which do not pass close to the fixed point and unstable manifold, or which oscillate about the unstable manifold. In this case, we cannot be confident that the numerical solution is giving a good approximation to the attractor or the dynamics on it.

To overcome these difficulties, a new error control, the phase space $\theta(\mathrm{PS}_\theta)$ error control, was introduced in [9]. In this error control,the numerical solution $\{y_n\}_{n=0}^\infty$ satisfies the constraint

$$\|y_{n+1} - y_n - h_n[(1-\theta)f(y_n) + \theta f(y_{n+1})]\| \leqslant \varphi h_n \|(1-\theta)f(y_n) + \theta f(y_{n+1})\|, \tag{2}$$

at every step, where $\varphi \in (0,1)$ is a user defined parameter akin to a tolerance, and $\theta \in [0,1]$ is also a parameter to be chosen. This is a generalization of the PS error control introduced in [8], which corresponded to (2) with $\theta = 1/2$. It was seen in [9] that this error control automatically controls the step-size relative to the stability limit.Although the PS_θ constraint is applicable to arbitrary numerical method, we will concentrate on its use with embedded Runge-Kutta pairs.

Next,we outline the traditional standard error control which performs badly near fixed points as mentioned above, and we illustrate these performances in sections 4.1 and 4.2 and we see that how these are removed by the addition of the PS_θ constraint.

Most of the ideas in this work apply to general variable time-stepping algorithms. In order to state precise results, we focus on embedded explicit Runge-Kutta (ERK) pairs. The main details of a typical adaptive ERK algorithm of the type available in numerical software libraries are described below. Further details of these methods can be found, for example, in [3, 10].

Let t_n denote sequence of unequally spaced grid points in time and y_n denote an approximation of $y(t_n)$ of (1.1) and h_n a step-size at t_n such that $h_n = t_{n+1} - t_n$ and $t_n = \sum_{j=0}^{n-1} h_j$. Given y_n and h_n, the ERK pair is defined as follows: An embedded Runge-Kutta pair is defined by

$$Y_i = y_n + h_n \sum_{j=1}^{i-1} a_{ij} f(Y_j), \qquad 1 \leqslant i \leqslant s. \tag{3}$$

$$y_{n+1} = y_n + h_n \sum_{i=1}^{s} b_i f(Y_i), \tag{4}$$

$$\widetilde{y}_{n+1} = y_n + h_n \sum_{i=1}^{s} \widetilde{b}_i f(Y_i). \tag{5}$$

Here $\{a_{ij}, b_i, \widetilde{b}_i\}, 1 \leqslant j \leqslant i-1 , 1 \leqslant i \leqslant s$ are the coefficients of the ERK pair. In equation (4), y_{n+1} gives an approximation to the solution $y(t_{n+1})$ of (1.1) whereas $\widetilde{y}_{n+1}$, obtained from (5), is used only for local error estimation and step-size selection. The coefficients $\{a_{ij}, b_i, \widetilde{b}_i\}, 1 \leqslant j \leqslant i-1, 1 \leqslant i \leqslant s$, of the above ERK pair are usually represented by the Butcher array

$$\begin{array}{c|c} & A \\ \hline & b \\ & \widetilde{b} \end{array}.$$

Equations (3)-(5) are denoted by $RKp(q)$, where p is the order of the method using Y_i and y_{n+1}, and $q(\neq p)$ is the order of the method using Y_i and $\widetilde{y}_{n+1}$. If $p > q$, then the method is said to be in *extrapolation mode*. Otherwise, it is said to be in *non-extrapolation mode*. In general, either $p = q + 1$ or $q = p + 1$.

In typical local error control, the difference $y_{n+1} - \widetilde{y}_{n+1}$ yields an estimate of the local error which can be used to alter the step-size during integration. An estimate of the local error is bounded at each time-step by a user-defined tolerance τ which allows the step-size to either increase or decrease over the next step. Let

$$E(y_n, h_n) = \frac{1}{h_n^\rho}(y_{n+1} - \widetilde{y}_{n+1}), \tag{6}$$

be an approximation to the local truncation error over a step with $\rho = 0$ (Error-Per-Step (EPS)) or with $\rho = 1$ (Error-Per-Unit-Step (EPUS)). The error estimate $\|E(y_n, h_n)\|$ is used for two purposes, error control and step-size selection. For both cases(EPS & EPUS), the step-size h_n is chosen at each step such that

$$\|E(y_n, h_n)\| \leqslant \tau, \tag{7}$$

where $0 < \tau \ll 1$. In this case an approximation y_{n+1} is regarded as acceptable, otherwise the step-size is rejected and re-computed with smaller step-size until the constraint (7) becomes true. The standard formula for the next step is

$$h_{n+1} = \left(\frac{\gamma\tau}{\|E(y_n, h_n)\|}\right)^{1/\overline{q}} h_n, \tag{8}$$

where $\overline{q}$ is the largest integer such that $\|E(y_n, h_n)\| = \mathcal{O}(h_n^{\overline{q}})$. So, $\overline{q} = \min(p, q) + 1 - \rho$. The constant safety factor $\gamma \in (0, 1)$ is included to avoid rejecting too many steps. Values of γ between 0.8 and 0.9 are typical.

In the next section, we discuss the behavior of the forward Euler method with PS_θ error control(2) when applied to linear systems. In particular, for linear system, whose coefficient matrix has eigenvalues which are real and negative, with a stable hyperbolic fixed point, it is shown that this error control gives a numerical solution which is forced to converge to the fixed point. In section 3, the new step-size selection scheme is introduced and step-size stability is discussed. In particular, we show that, in the neighborhood of fixed point, the step-size h_n tends a constant value when PS_θ error control applied to the system of ODEs (1). In section 4, we present some numerical simulations which illustrate and confirm our analysis, as regards the dynamics of the numerical solutions and step-size sequences near fixed points. The work is summarized in section 5.

2 Linear System

In this section, we restrict to discuss the behavior of the forward Euler method under PS_θ error control (2) when applied to the linear system

$$y_t = Ay, \quad y(0) = y_0 \in \mathbb{R}^m \tag{9}$$

with real $m \times m$ matrix A.

When the forward Euler method is applied to the above system (9), the numerical solution $\{y^n\}$ evolves according to

$$y^{n+1} = R(h_n A)y^n, \tag{10}$$

where $R(h_n A)$ is the stability polynomial matrix given by

$$R(h_n A) = I + h_n A. \tag{11}$$

With (10) the PS$_\theta$ constraint (2) becomes

$$\|R(h_n A) - 1 - h_n[(1-\theta)A + \theta A R(h_n A)]y^n\| \leqslant \varphi h_n \|[(1-\theta)A + \theta A R(h_n A)]y^n\|, \qquad (12)$$

for any vector norm $\|\cdot\|$.

We require the following theorem in order to discuss the behavior of the forward Euler method applied to the system (9) under PS$_\theta$ control (2).

Theorem 2.1 *Consider the forward Euler method under PS$_\theta$ error control (2) in $\|\cdot\|_\infty$ with $\varphi < \theta/(1-\theta)$ applied to the system*

$$y_t = \Lambda y, \quad \Lambda = \mathrm{Diag}[\lambda_1, \lambda_2, \ldots, \lambda_m], \quad \lambda_i < 0 \,\forall i, \quad y(0) = y^0 \in \mathbb{R}^m \qquad (13)$$

with $\lambda_1 < \lambda_2 < \ldots < \lambda_{m-1} < \lambda_m < 0$, and the initial conditions satisfy $y(0) = y^0 = [y_1^0, \ldots, y_m^0] \in \mathbb{R}^m$ with $y_m^0 \neq 0$. Then $\|y^n\|_\infty \to 0$ as $n \to \infty$ with the following:

1. *$y_m^n \to 0$ monotonically as $n \to \infty$;*

2. *If $\lambda_i \geqslant \frac{\theta(1+\varphi)}{\varphi}\lambda_m$ then $y_i^n \to 0$ and $\frac{y_i^n}{y_m^n} \to 0$ both monotonically as $n \to \infty$;*

3. *If $\frac{\theta(1+\varphi)}{\varphi}\lambda_m > \lambda_i \geqslant \left[\frac{2\theta(1+\varphi)}{\varphi} - 1\right]\lambda_m$ then $y_i^n \to 0$ and $\left|\frac{y_i^n}{y_m^n}\right| \to 0$ as $n \to \infty$;*

4. *For all remaining components of y^n, we have $y_i^n \to 0$ as $n \to \infty$ with*

$$\limsup_{n \to \infty} \left|\frac{y_i^n}{y_m^n}\right| < \frac{\varphi}{\theta - \frac{\varphi}{1+\varphi}};$$

5. *Let θ_n be the angle between y^n and $[0, 0, \cdots, 0, 1] \in \mathbb{R}^m$. Then*

$$\liminf_{n \to \infty} \cos \theta_n \geqslant \frac{1}{\sqrt{1 + (m-1)\left(\frac{\varphi}{\theta - \frac{\varphi}{1+\varphi}}\right)^2}} \geqslant 1 - \frac{1}{2}(m-1)\frac{\varphi^2}{\theta^2} + \mathcal{O}(\varphi^3).$$

Proof. For the system (13), the stability polynomial matrix $R(h_n A)$ given by (11) is a diagonal matrix which is expressed as

$$R(h_n A) \quad = \quad \mathrm{Diag}[1 + h_n\lambda_1, 1 + h_n\lambda_2, \cdots, 1 + h_n\lambda_m]. \qquad (14)$$

With the ∞-norm, $\|\cdot\|_\infty$, from (12), (14) we have

$$\left\|\begin{bmatrix} -\theta h_n^2 \lambda_1^2 y_1^n \\ -\theta h_n^2 \lambda_2^2 y_2^n \\ \vdots \\ -\theta h_n^2 \lambda_m^2 y_m^n \end{bmatrix}\right\|_\infty \quad \leqslant \quad \varphi h_n \left\|\begin{bmatrix} \lambda_1(1 + \theta\lambda_1 h_n)y_1^n \\ \lambda_2(1 + \theta\lambda_2 h_n)y_2^n \\ \vdots \\ \lambda_m(1 + \theta\lambda_m h_n)y_m^n \end{bmatrix}\right\|_\infty. \qquad (15)$$

This implies that at least one of the following

$$h_n \theta \lambda_i^2 |y_i^n| \quad \leqslant \quad -\varphi\lambda_i|1 + \theta\lambda_i h_n||y_i^n|, \ i = 1, 2, \cdots, m \qquad (16)$$

must hold. Since $h_n > 0$, the above constraint (16) implies that the ith inequality of (16) holds if and only if

$$h_n \leqslant -\frac{\varphi}{\lambda_i\theta(1+\varphi)}, \ i = 1, 2\cdots, m.$$

Since

$$-\frac{\varphi}{\lambda_i(1+\varphi)} \leqslant -\frac{\varphi}{\lambda_m(1+\varphi)}, \ i = 1, 2, \cdots, m$$

and one of (16) holds, $h_n \leqslant -\varphi/\lambda_m\theta(1+\varphi)$ for every step h_n satisfying PS$_\theta$ error constraint (2), and so (16) is satisfied with $i = m$ at every step. Since $\varphi < \theta/1 - \theta$, it follows that $h_n < -\frac{1}{\lambda_m}$ for every step h_n satisfying PS$_\theta$ error constraint (2). Now consider the evolution of y_m^n. From (10), we obtain

$$y_m^{n+1} = (1 + h_n\lambda_m)y_m^n. \tag{17}$$

Since $0 < 1 + h_n\lambda_m < 1$ for every step h_n satisfying (2), it follows from (17) that $y_m^n \to 0$ monotonically as $n \to \infty$.

Suppose that the ith inequality of (16) holds. Then by Theorem 5.2 of [9], $0 < 1 + h_n\lambda_i < 1$. Now consider the evolution

$$y_i^{n+1} = (1 + h_n\lambda_i)y_i^n, \tag{18}$$
$$y_m^{n+1} = (1 + h_n\lambda_m)y_m^n. \tag{19}$$

It follows from (18) and (19) that

$$\frac{\left|y_i^{n+1}\right|}{\left|y_m^{n+1}\right|} = \frac{1 + h_n\lambda_i}{1 + h_n\lambda_m}\frac{\left|y_i^n\right|}{\left|y_m^n\right|}$$

which gives

$$\frac{\left|y_i^{n+1}\right|}{\left|y_m^{n+1}\right|} < \frac{\left|y_i^n\right|}{\left|y_m^n\right|}$$

since $\lambda_i < \lambda_m$. That is, the ratio $\frac{|y_i^n|}{|y_m^n|}$, $i < m$, decreases at any step for which ith inequality of (16) holds. Since $1 + h_n\lambda_i > 0$ and $1 + h_n\lambda_m > 0$,

$$\text{Sign}\left\{\frac{y_i^{n+1}}{y_m^{n+1}}\right\} = \text{Sign}\left\{\frac{y_i^n}{y_m^n}\right\}.$$

Suppose that the ith inequality of (16) fails and jth component of the right hand side of (15) gives $\|\cdot\|_\infty$. Then

$$-\frac{\varphi}{\lambda_i\theta(1+\varphi)} < h_n \leqslant -\frac{\varphi}{\lambda_j\theta(1+\varphi)}. \tag{20}$$

From (15), we have

$$h_n\theta\lambda_i^2|y_i^n| \leqslant -\varphi\lambda_j|1 + \theta\lambda_j h_n||y_j^n|. \tag{21}$$

Since $h_n \leqslant -\frac{\varphi}{\lambda_j\theta(1+\varphi)}$, $1 + h_n\theta\lambda_j > 0$. Thus the constraint (21) gives

$$|y_i^n| \leqslant -\frac{\varphi\lambda_j}{h_n\theta\lambda_i^2}(1 + \theta\lambda_j h_n)\left|y_j^n\right|. \tag{22}$$

Since $-\frac{\varphi}{\lambda_j\theta(1+\varphi)} < h_n$, it follows from (22) that

$$|y_i^n| < -\varphi\lambda_j\frac{\left(1 - \frac{\lambda_j}{\lambda_i}\frac{\varphi}{1+\varphi}\right)}{\lambda_i^2\frac{\varphi}{(-\lambda_i)(1+\varphi)}}\left|y_j^n\right| = \frac{\lambda_j}{\lambda_i}\left(1 + \varphi - \frac{\lambda_j}{\lambda_i}\varphi\right)\left|y_j^n\right| < \frac{\lambda_j}{\lambda_i}(1+\varphi)|y_j^n|. \tag{23}$$

Now consider the evolution at the next step

$$y_i^{n+1} = (1 + \lambda_i h_n)y_i^n, \tag{24}$$
$$y_j^{n+1} = (1 + \lambda_j h_n)y_j^n. \tag{25}$$

It follows from (24) and (25) that

$$\frac{\left|y_i^{n+1}\right|}{\left|y_j^{n+1}\right|} = \frac{|1 + \lambda_i h_n|}{(1 + \lambda_j h_n)}\frac{\left|y_i^n\right|}{\left|y_j^n\right|}. \tag{26}$$

Let

$$F(h_n) = \frac{1 + \lambda_i h_n}{1 + \lambda_j h_n}. \tag{27}$$

This implies that

$$F'(h_n) = \frac{\lambda_i - \lambda_j}{(1 + \lambda_j h_n)^2} < 0$$

and hence F is decreasing function of h_n. Since $F(0) = 1$, it follows that $F(h_n) < 1 \; \forall \; h_n > 0$. Then by (20)

$$|F(h_n)| \leqslant \max\left\{\left|F\left(-\frac{\varphi}{\lambda_i \theta(1+\varphi)}\right)\right|, \left|F\left(-\frac{\varphi}{\lambda_j \theta(1+\varphi)}\right)\right|\right\}. \tag{28}$$

Now, consider two cases.

Case (i) $\lambda_i \geqslant \frac{\theta(1+\varphi)}{\varphi}\lambda_m$

In this case, we have $1 + h_n\lambda_i > 0$. Since, clearly $1 + h_n\lambda_i < 1$, it follows from (18) and (24) that $y_i^n \to 0$ monotonically as $n \to \infty$ whether or not the ith inequality of (16) holds. Further, we have

$$F\left(-\frac{\varphi}{\lambda_j \theta(1+\varphi)}\right) = \frac{\theta(1+\varphi) - \frac{\lambda_i}{\lambda_j}\varphi}{\theta(1+\varphi) - \varphi} > 0$$

which gives $0 < F(h_n) < 1 \; \forall \; h_n$ satisfying (20). Hence from (26) and (27), we obtain that the ratio $\frac{|y_i^n|}{|y_j^n|}$ decreases at any step in which ith inequality of (16) fails. Since jth constraint of (16) holds, we obtain that the ratio $\frac{|y_j^n|}{|y_m^n|}$ decreases as before. Thus the ratio $\frac{|y_i^n|}{|y_m^n|}$ decreases at any step for which ith inequality of (16) fails and hence the ratio $\frac{y_i^n}{y_m^n} \to 0$ monotonically as $n \to \infty$ whether or not the ith inequality holds.

Case (ii) $\frac{\theta(1+\varphi)}{\varphi}\lambda_m > \lambda_i \geqslant \left[\frac{2\theta(1+\varphi)}{\varphi} - 1\right]\lambda_m$

In this case we have

$$\frac{\lambda_i}{\lambda_m} \leqslant \frac{2\theta(1+\varphi)}{\varphi} - 1.$$

$\Rightarrow$

$$\frac{\lambda_i}{\lambda_j} \leqslant \frac{2\theta(1+\varphi)}{\varphi} - 1.$$

$\Rightarrow$

$$\frac{\lambda_i}{\lambda_j} - \frac{\theta(1+\varphi)}{\varphi} \leqslant \frac{\theta(1+\varphi)}{\varphi} - 1. \tag{29}$$

This implies that

$$F\left(-\frac{\varphi}{\lambda_j \theta(1+\varphi)}\right) = \frac{\theta(1+\varphi) - \frac{\lambda_i}{\lambda_j}\varphi}{\theta(1+\varphi) - \varphi} > -1.$$

Thus $-1 < F(h_n) < 1 \; \forall \; h_n$ satisfying (20). It follows from (26) and (27) that the ratio $\frac{|y_i^n|}{|y_j^n|}$ decreases. Since the ratio $\frac{|y_j^n|}{|y_m^n|}$ also decreases, it follows that the ratio $\frac{|y_i^n|}{|y_m^n|}$ decreases and hence $\frac{|y_i^n|}{|y_m^n|} \to 0$ as $n \to \infty$. Since $y_m^n \to 0$ monotonically, it follows that $y_i^n \to 0$ as $n \to \infty$.

For all remaining components of y^n, there are two cases.

If $\frac{\lambda_i}{\lambda_j} \leqslant \frac{2\theta(1+\varphi)}{\varphi} - 1 < \frac{\lambda_i}{\lambda_m}$, it can be shown that $-1 < F(h_n) < 1 \; \forall \; h_n$ satisfying (20). Hence the result follows from case(ii).

If $\frac{2\theta(1+\varphi)}{\varphi} - 1 < \frac{\lambda_i}{\lambda_j} \leqslant \frac{\lambda_i}{\lambda_m}$, then

$$F\left(-\frac{\varphi}{\lambda_j \theta(1+\varphi)}\right) = \frac{\theta(1+\varphi) - \frac{\lambda_i}{\lambda_j}\varphi}{\theta(1+\varphi) - \varphi} < -1. \tag{30}$$

Thus from (23), (26), (27), (28), (30) we obtain that

$$
\begin{aligned}
\frac{|y_i^{n+1}|}{|y_j^{n+1}|} &\leqslant \left(\frac{\frac{\lambda_i}{\lambda_j}\frac{\varphi}{\theta(1+\varphi)} - 1}{1 - \frac{\varphi}{\theta(1+\varphi)}} \right) \frac{\lambda_j}{\lambda_i}(1+\varphi) \\
&= \frac{\frac{\varphi}{\theta} - \frac{\lambda_j}{\lambda_i}(1+\varphi)}{1 - \frac{\varphi}{\theta(1+\varphi)}} \\
&< \frac{\frac{\varphi}{\theta}}{1 - \frac{\varphi}{\theta(1+\varphi)}} \\
&= \frac{\varphi}{\theta - \frac{\varphi}{1+\varphi}}.
\end{aligned}
\tag{31}
$$

Since the ratio $\frac{|y_j^n|}{|y_m^n|} \to 0$ as $n \to \infty$, for large n,

$$
\frac{|y_j^{n+1}|}{|y_m^{n+1}|} < 1.
\tag{32}
$$

Thus from (31) and (32), we have

$$
\frac{|y_i^{n+1}|}{|y_m^{n+1}|} < \frac{\varphi}{\theta - \frac{\varphi}{1+\varphi}}
$$

for large n. Hence the result 4 follows.

Let θ_n be the angle between y^n and $[0, 0, \ldots, 0, 1] \in \mathbb{R}^m$. Then

$$
\cos\theta_n = \frac{|y_m^n|}{\sqrt{\sum_{i=1}^m (y_i^n)^2}} = \frac{1}{\sqrt{\sum_{i=1}^m (y_i^n/y_m^n)^2}}.
$$

Hence

$$
\begin{aligned}
\liminf_{n\to\infty} \cos\theta_n &= \frac{1}{\limsup_{n\to\infty} \sqrt{\sum_{i=1}^m (y_i^n/y_m^n)^2}} \\
&\geqslant \frac{1}{\sqrt{\sum_{i=1}^m \limsup_{n\to\infty}(y_i^n/y_m^n)^2}} = \frac{1}{\sqrt{1 + \sum_{i=1}^{m-1} \limsup_{n\to\infty}(y_i^n/y_m^n)^2}}
\end{aligned}
$$

It follows from the result (4) that

$$
\begin{aligned}
\liminf_{n\to\infty} \cos\theta_n &\geqslant \frac{1}{\sqrt{1 + \sum_{i=1}^{m-1}\left(\frac{\varphi}{\theta - \frac{\varphi}{1+\varphi}}\right)^2}} \\
&= \left[1 + (m-1)\varphi^2(1+\varphi)^2(\theta - (1-\theta)\varphi)^{-2}\right]^{-1/2} \\
&= \left[1 + (m-1)\frac{\varphi^2}{\theta^2}(1+\varphi)^2\left(1 - (1-\theta)\frac{\varphi}{\theta}\right)^{-2}\right]^{-1/2} \\
&= \left[1 + (m-1)\frac{\varphi^2}{\theta^2}(1+\varphi)^2\left(1 + 2(1-\theta)\frac{\varphi}{\theta} + \mathcal{O}(\varphi^2)\right)\right]^{-1/2} \\
&= \left[1 + (m-1)\frac{\varphi^2}{\theta^2} + \mathcal{O}(\varphi^3)\right]^{-1/2} \\
&= 1 - \frac{1}{2}(m-1)\frac{\varphi^2}{\theta^2} + \mathcal{O}(\varphi^3).
\end{aligned}
$$

Hence the result (5) follows.   □

Note that the bound in (4) is independent of the stiffness/eigenvalues of the system and it can be made arbitrarily small by reducing φ. In result (5), note that the exact solution will be tangent to $[0, 0, \cdots, 0, 1]$ at the fixed point, so this result gives us a bound on the angle between the exact and numerical solutions at the fixed point. By reducing φ, we can make the angle arbitrarily small(independent of the stiffness/eigenvalues).

Remark This results are extended to arbitrary norms and to non-diagonal linear system in the following theorem.

Theorem 2.2 *Consider the forward Euler method under PS_θ error control (2) with sufficiently small φ applied to the system (9) where the matrix A is diagonalizable with real negative eigenvalues λ_i, $i = 1, 2, \cdots, m$, satisfying $\lambda_1 < \lambda_2 < \cdots < \lambda_{m-1} < \lambda_m < 0$. Then $\|y^n\| \to 0$ as $n \to \infty$.*

Proof. Since the matrix A is diagonalisable, there exists a non-singular matrix P such that $P^{-1}AP = D$ a diagonal matrix whose diagonal entries are $\lambda_1, \lambda_2, \cdots, \lambda_m$. Then the stability polynomial matrix $R(h_nA)$ given by (11) satisfies

$$P^{-1}R(h_nA)P = \text{Diag}[1 + h_n\lambda_1, 1 + h_n\lambda_2, \cdots, 1 + h_n\lambda_m] = \overline{R}(h_nD)(\text{Say}). \tag{33}$$

With (33), the inequality (12) becomes,

$$\|P\{\overline{R}(h_nD) - I - h_n[(1-\theta)D + \theta D\overline{R}(h_nD)]\}z^n\| \leqslant \varphi h_n\|P[(1-\theta)D + \theta D\overline{R}(h_nD)]z^n\| \tag{34}$$

where $z^n = P^{-1}y^n$. Now we define a new norm $\|\cdot\|_P$ by

$$\|x\|_P = \|Px\|, \quad \forall x \in \mathbb{R}^m. \tag{35}$$

With this norm, the constraint (34) becomes

$$\left\|\{\overline{R}(h_nD) - I - h_n[(1-\theta)D + \theta D\overline{R}(h_nD)]\}z^n\right\|_P \leqslant \varphi h_n\left\|[(1-\theta)D + \theta D\overline{R}(h_nD)]z^n\right\|_P. \tag{36}$$

Since norms are equivalent on a finite dimensional linear space, $\exists c_1, c_2 > 0$ such that

$$c_1\|x\|_\infty \leqslant \|x\|_P \leqslant c_2\|x\|_\infty \quad \forall x \in \mathbb{R}^m. \tag{37}$$

By combining (36) and (37), we obtain

$$\left\|\{\overline{R}(h_nD) - I - h_n[(1-\theta)D + \theta D\overline{R}(h_nD)]\}z^n\right\|_\infty \leqslant \varphi\left(\frac{c_2}{c_1}\right)h_n\left\|[(1-\theta)D + \theta D\overline{R}(h_nD)]z^n\right\|_\infty. \tag{38}$$

This gives

$$\left\|\begin{bmatrix} -\theta h_n^2\lambda_1^2 z_1^n \\ -\theta h_n^2\lambda_2^2 z_2^n \\ \vdots \\ -\theta h_n^2\lambda_m^2 z_m^n \end{bmatrix}\right\|_\infty \leqslant \varphi_1 h_n \left\|\begin{bmatrix} \lambda_1(1 + \theta\lambda_1 h_n)z_1^n \\ \lambda_2(1 + \theta\lambda_2 h_n)z_2^n \\ \vdots \\ \lambda_m(1 + \theta\lambda_m h_n)z_m^n \end{bmatrix}\right\|_\infty. \tag{39}$$

where $\varphi_1 = \varphi\left(\frac{c_2}{c_1}\right)(< 1$ for sufficiently small φ.) This implies that at least one of the following

$$h_n\theta\lambda_i^2|z_i^n| \leqslant -\varphi_1\lambda_i|1 + \theta\lambda_i h_n||z_i^n|, \ i = 1, 2, \cdots, m \tag{40}$$

must hold. Since φ is sufficiently small, we can choose φ so that $\varphi < \frac{c_1}{c_2}\frac{\theta}{1-\theta}$ giving $\varphi_1 < \frac{\theta}{1-\theta}$. Hence by theorem (2.1), we obtain that $\|z^n\| \to 0$ as $n \to \infty$. This implies that $\|y^n\| \to 0$ as $n \to \infty$ for any norm $\|\cdot\|$ since $y^n = Pz^n$ and P is non-singular.

$\square$

3 Step-size selection and step-size stability

3.1 Step-size selection

The step-size selection strategies used in [8, 9] are not entirely satisfactory. So, we introduce a new step-size strategy based on step-sizes derived from the standard error control and PS_θ error control respectively. First, we derive the step-size which satisfies the PS_θ constraint(2). This step-size can be combined with the step-size obtained from the standard algorithm in order to select a new step-size. Let

$$R(y_n, h_n) = \frac{\|y_{n+1} - y_n - h_n[(1-\theta)f(y_n) + \theta f(y_{n+1})]\|}{h_n\|(1-\theta)f(y_n) + \theta f(y_{n+1})\|}. \tag{41}$$

Now suppose the numerical solutions $\{y_n\}$ is generated by a method of order p and let $u(t)$ be an exact solution of the ODEs (1) with initial condition perturbed so that $u(t_n) = y_n$. Then

$$
\begin{aligned}
y_{n+1} - y_n &- h_n\left[(1-\theta)f(y_n) + \theta f(y_{n+1})\right] \\
&= \left[u(t_{n+1}) + \mathcal{O}(h_n^{p+1})\right] - u(t_n) - h_n\left[(1-\theta)f(u(t_n)) + \theta[f(u(t_{n+1})) + \mathcal{O}(h_n^{p+1})]\right] \\
&= u(t_{n+1}) - u(t_n) - h_n\left[(1-\theta)f(u(t_n)) + \theta f(u(t_{n+1}))\right] + \mathcal{O}(h_n^{p+1}) \\
&= \mathcal{L}_\theta(u(t_{n+1})) + \mathcal{O}(h_n^{p+1})
\end{aligned}
$$

where $\mathcal{L}_\theta$ is the local truncation error of the θ-method. Hence

$$y_{n+1} - y_n - h_n\left[(1-\theta)f(y_n) + \theta f(y_{n+1})\right] = \mathcal{O}(h_n^{r+1}) + \mathcal{O}(h_n^{p+1})$$

where $r = 2$ if $\theta = 1/2$ and $r = 1$ otherwise. Hence from (41), we have

$$R(y_n, h_n) = \frac{\|\mathcal{O}(h_n^{\tilde{q}+1})\|}{h_n\|f(y_n) + \mathcal{O}(h_n)\|} = \frac{\|h_n^{\tilde{q}+1}\psi(y_n) + \mathcal{O}(h_n^{\tilde{q}+2})\|}{h_n\|f(y_n) + \mathcal{O}(h_n)\|} = \frac{h_n^{\tilde{q}}\|\psi(y_n)\|}{\|f(y_n)\|} + \mathcal{O}(h_n^{\tilde{q}+1}) \quad (42)$$

where $\psi(\cdot)$ is a function of f and its derivatives at y_n, and $\tilde{q} \geqslant \min(p, r)$ with $\tilde{q} = \min(p, r)$ if $p \neq r$. Thus

1. Method (4) of order $p = 1$ and $\theta = 1/2$ implies $\tilde{q} = 1$;

2. Method (4) of order $p = 2$ and $\theta = 1/2$ implies $\tilde{q} \geqslant 1$;

3. Method (4) of order $p \geqslant 2$ and $\theta \neq 1/2$ implies $\tilde{q} = 1$;

4. Method (4) of order $p \geqslant 3$ and $\theta = 1/2$ implies $\tilde{q} = 2$.

Other cases can be computed using Taylor series expansions.

Now, when advancing from t_n to t_{n+1}, we want to choose a step-size h_{n+1} to satisfy the constraint $R(y_{n+1}, h_{n+1}) \leqslant \varphi$. To achieve this, we require that

$$R(y_{n+1}, h_{n+1}) \approx \chi\varphi, \tag{43}$$

where $\chi \in (0, 1)$ is a constant safety factor. By approximating

$$\frac{|\psi(y_{n+1})\|}{\|f(y_{n+1})\|} \approx \frac{\|\psi(y_n)\|}{\|f(y_n)\|},$$

we obtain from (42) that

$$\frac{R(y_{n+1}, h_{n+1})}{R(y_n, h_n)} = \left(\frac{h_{n+1}}{h_n}\right)^{\tilde{q}}. \tag{44}$$

It follows from (43) that

$$h_{n+1} = \left(\frac{\chi\varphi}{R(y_n, h_n)}\right)^{1/\tilde{q}} h_n. \tag{45}$$

We now describe in detail the strategy for computing the new step-size, h_{new}, from the step-sizes derived from the standard error control and the PS_θ error control. Consecutive step-sizes must satisfy $h_{n+1} \leqslant \alpha h_n$; this restricts the relative increase of the step-size over each step, where α is a *maximum step-size ratio* which is set at $\alpha = 5$. It is also common to impose a maximum step-size, $h_{\max}$, so that $h_n \leqslant h_{\max}$ for all n. Thus, using the formulae (8) and (45) we calculate

$$h_{n+1}^S = \left(\frac{\gamma \tau}{\|E(y_n, h_n)\|} \right)^{1/\overline{q}} h_n, \tag{46}$$

$$h_{n+1}^\theta = \left(\frac{\chi \varphi}{R(y_n, h_n)} \right)^{1/\widetilde{q}} h_n, \tag{47}$$

and compute

$$h_{new} = \min\{h_{n+1}^S, h_{n+1}^\theta, \alpha h_n, h_{\max}\}. \tag{48}$$

3.2   Step-size stability

In this section, we show that, in the neighborhood of fixed point, the step-size h_n tends to a constant value when PS_θ constraint applied to the initial value problem (1). For the numerical solution is driven to be fixed point by our algorithm, we require that in a neighborhood of the fixed point at every step, the step-sizes are chosen in (48) according to the step-size given by (47).

Thus, in near fixed point, the evolution of the step-size will be determined by

$$h_{n+1} = \left(\frac{\chi \varphi}{R(y_n, h_n)} \right)^{1/\widetilde{q}} h_n := \mathcal{G}(h_n), \tag{49}$$

provided $R(y_n, h_n) \leqslant \varphi$,   where $R(y_n, h_n)$ is given by (41). This iteration (49) has a fixed point $h^* = \mathcal{G}(h^*)$ at h^* such that $R(y_n, h^*) = \gamma_1 \varphi$. For this iteration to be stable, we require that $|\mathcal{G}'(h^*)| < 1$, with quadratic convergence if $\mathcal{G}'(h^*) = 0$. We will now show that convergence of this iteration can be achieved with quadratic convergence in the limit as $\varphi \to 0$.

From (49), we have

$$\begin{aligned} \mathcal{G}'(h^*) &= \left(\frac{\chi \varphi}{R(y_n, h^*)} \right)^{1/\widetilde{q}} - \frac{h^*}{\widetilde{q}} \left(\frac{\chi \varphi}{R(y_n, h^*)} \right)^{(1/\widetilde{q})-1} \frac{\chi \varphi}{R(y_n, h^*)^2} R_h(y_n, h^*) \\ &= 1 - \frac{h^*}{\widetilde{q}} \frac{1}{R(y_n, h^*)} R_h(y_n, h^*). \end{aligned} \tag{50}$$

where $R_h(\cdot, \cdot)$ denotes the derivative of R with respect to h. Equation (42) implies that

$$R_h(y_n, h) = \widetilde{q} \frac{\|\psi(y_n)\|}{\|f(y_n)\|} h^{\widetilde{q}-1} + \mathcal{O}(h^{\widetilde{q}}). \tag{51}$$

From (50),(42),(51), we have

$$\mathcal{G}'(h^*) = 1 - (1 + \mathcal{O}(h^*)) = \mathcal{O}(h^*). \tag{52}$$

Since $R(y_n, h^*) = \chi \varphi$, from (42), we have

$$\mathcal{O}((h^*)^{\widetilde{q}}) = \chi \varphi. \tag{53}$$

Hence from (52) and (53),   we obtain

$$\mathcal{G}'(h^*) = \mathcal{O}\left((\chi \varphi)^{1/\widetilde{q}} \right). \tag{54}$$

Thus, we expect that the step-size $h_n \to h^*$ in the neighborhood of a fixed point with quadratic convergence as $\varphi \to 0$. We now illustrate this approximate analysis by considering the following example. Consider the forward Euler method applied to the scalar linear problem

$$y_t = \lambda y, \quad y(0) = y_0 \in \mathbb{R} \tag{55}$$

with $\lambda < 0$. Since this method is of order 1, we have $\widetilde{q} = 1$. From (41), we have

$$R(h) = \frac{|\theta h \lambda|}{|1 + \theta h \lambda|} = \pm \frac{\theta h \lambda}{1 + \theta h \lambda}. \tag{56}$$

If $R(h) = \dfrac{\theta h \lambda}{1 + \theta h \lambda}$, then from (49) the fixed point h^* satisfies $R(h^*) = \chi\varphi$, we have

$$\chi\varphi = \frac{\theta h^* \lambda}{1 + \theta h^* \lambda}. \tag{57}$$

This gives

$$\theta h^* = \frac{\chi\varphi}{\lambda(1 - \chi\varphi)} < 0, \tag{58}$$

a contradiction. Thus

$$R(h) = -\frac{\theta h \lambda}{1 + \theta h \lambda}. \tag{59}$$

This implies that

$$R'(h) = -\frac{\theta \lambda}{(1 + \theta \lambda)^2}. \tag{60}$$

Since $R(h^*) = \chi\varphi$, from (59), we have

$$\theta h^* \lambda = -\frac{\chi\varphi}{1 + \chi\varphi} \tag{61}$$

and hence

$$1 + \theta h^* \lambda = \frac{1}{1 + \chi\varphi}. \tag{62}$$

Thus, from (49), (59), (60) we have

$$\mathcal{G}'(h^*) = 1 + \frac{h^* \theta \lambda}{\widetilde{q}\chi\varphi}(1 + \chi\varphi)^2 = 1 - \frac{1}{\widetilde{q}\chi\varphi}\left(\frac{\chi\varphi}{1 + \chi\varphi}\right)(1 + \chi\varphi)^2 = 1 - \frac{1}{\widetilde{q}}(1 + \chi\varphi) = -\chi\varphi$$

since $\widetilde{q} = 1$. So if $\varphi = 0$, then $\mathcal{G}'(h^*) = 0$ and we obtain quadratic convergence of the step-size given by the iteration (49). Further, $-1 < \mathcal{G}'(h^*) < 0$ for all $\chi, \varphi \in (0,1)$, the step-size h_n converges to h^* for any $\chi \in (0,1)$ and for any $\varphi \in (0,1)$.

4 Numerical solutions and Step-size sequences

In this section, the efficiency of the PS_θ augmented algorithm with new step-size selection scheme is evaluated by carrying out a variety of numerical experiments. These results are compared with the results obtained by the standard adaptive algorithm. Results for some selected problems and methods are reported here and conclusions shown here have been found to be valid in general. The values of θ for each method given by [9] are used here for the corresponding methods.

4.1   Stable fixed point Example

We consider the forward Euler (RK12) method applied to the system

$$y_t = \begin{bmatrix} -5 & 0 \\ 0 & -1 \end{bmatrix} \begin{bmatrix} y_1 \\ y_2 \end{bmatrix}. \quad y = [y_1, y_2]^T \tag{63}$$

and $y(0) = [1, 10^{-4}]^T$. A typical adaptive algorithm as defined in Section 1 with $\tau = 10^{-2}$ produces the dynamics observed in Figure 1.
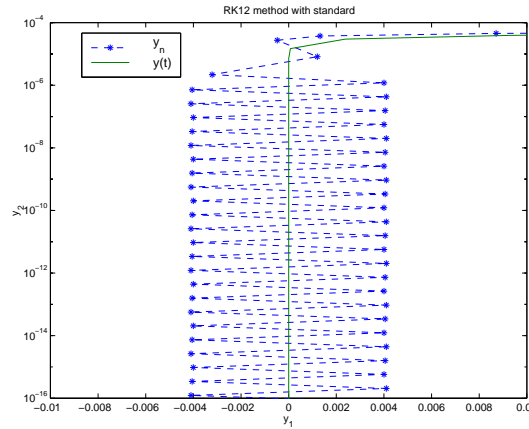

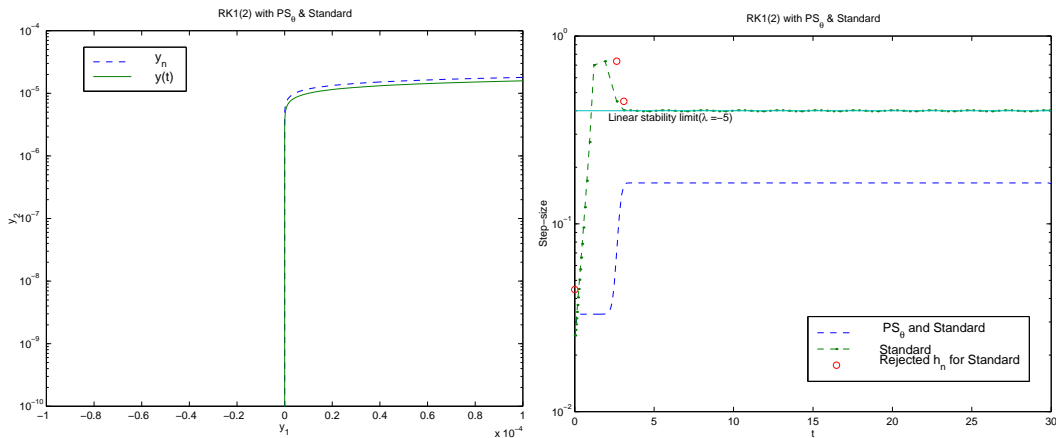**Fig. 1**   Numerical solutions of a typical adaptive algorithm near a stable fixed point for RK1(2).

Fig. 2   (i) Numerical solution using RK1(2) with PS$_\theta$ augmented algorithm around a stable fixed point. (ii) Step-sizes used by the typical and PS$_\theta$ augmented algorithms.

For the RK1(2) method the numerical solution gives a persistent spurious oscillation. Although the final solution is order of the tolerance from the fixed point, the spurious behavior persists for arbitrary small tolerances, and it is not possible to force the solution to converge to the fixed point.

If we now apply the RK1(2) method with PS$_\theta$ error control and $\varphi = 0.1$, we obtain the numerical solution in Figure 2(i), where we see that the numerical solution converges to the true fixed point. In Figure 2(ii) we show the step-size sequences used by the two algorithms. The typical adaptive algorithm has some step-size rejections, whilst the PS$_\theta$ algorithm has no rejections and quickly converges to a constant value.

4.2   Saddle point Example

We apply the RK2(3) and Fehlberg4(5) methods under standard adaptive error control to the system

$$y_t) = \begin{bmatrix} -1 & 0 \\ 0 & 1 \end{bmatrix} \begin{bmatrix} y_1 \\ y_2 \end{bmatrix}, \quad y = [y_1, y_2]^T \tag{64}$$

so that the origin is a saddle point, and take $y(0) = [0.99, 10^{-10}]^T$; very close to the stable manifold.
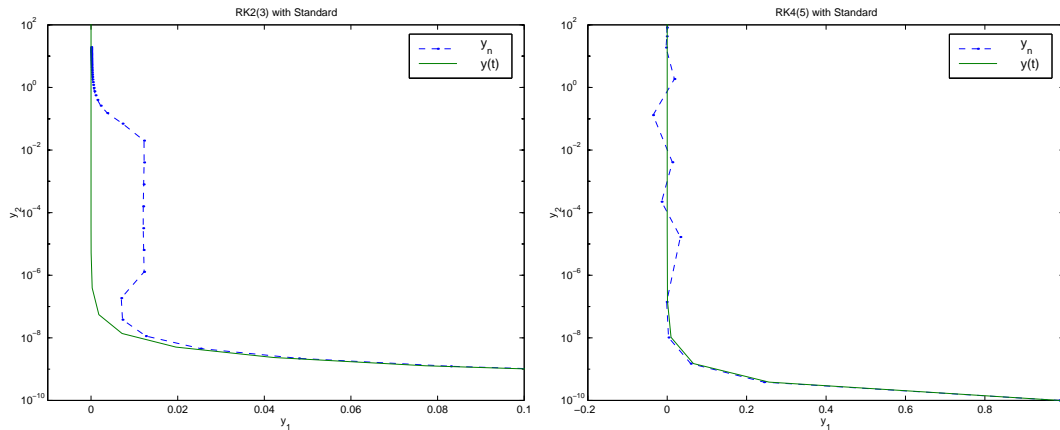

Fig. 3   Numerical solutions of a typical adaptive algorithm near a saddle point for (i) RK2(3), (ii) Fehlberg4(5).

For RK2(3) method, it is observed in the Figure 3(i) that the numerical solution does not pass as close to the fixed point or the local unstable manifold as it should, and there is also a significant phase difference between the exact and numerical solutions. As in the previous example this behavior persists for arbitrary small tolerances. For Fehlberg4(5) method, the numerical solution has a spurious oscillation about the unstable manifold, and although this oscillation decays as the solution moves away from the fixed point, the numerical solution can ultimately end up on either side of the unstable manifold depending on the exact initial condition; thus the property of the unstable manifold of the fixed point acting as a separatrix is lost by the numerical solution.

If we now apply the RK2(3) method under PS_θ augmented error control with $\varphi = 0.1$, we obtain the numerical solution in Figure 4(i), where we see that the numerical solution follows the exact solution very closely. In Figure 4(ii) we show the step-sizes used by the two algorithms. The PS_θ algorithm quickly settles to a constant step-size whilst the solution is near the local stable manifold then adjusts to a different constant step-size whilst the solution is near to the local unstable manifold. In contrast the poorer dynamical behavior of the typical adaptive algorithm results from the large step-sizes that it uses whilst the solution is near to the origin. Note that ultimately as y_2 becomes large the local error estimate determines and reduces the step-size in both algorithms; the different times at which it does so reveals the large phase shift introduced by the typical adaptive algorithm. Similar behavior is seen for the Fehlberg4(5) method in Figure 5.

4.3   Maximum step-size sequences

In this section, we plot the maximum acceptable step-sizes in phase space for both PS_θ and standard error controls in order to get the region in space where either one of these error controls determines the step-sizes. The maximum step-sizes occur when the error control(PS_θ or standard) is satisfied with equality. These maximum step-sizes are computed when numerical methods with these error controls are applied to the linear systems (63), (64) and the non-linear system, given by [4],

$$y_t = \begin{bmatrix} 2y_2 \\ 2y_1 - 3y_1^2 - y_2(y_1^3 - y_1^2 + y_2^2 - c) \end{bmatrix}, \quad y = [y_1, y_2]^T \tag{65}$$
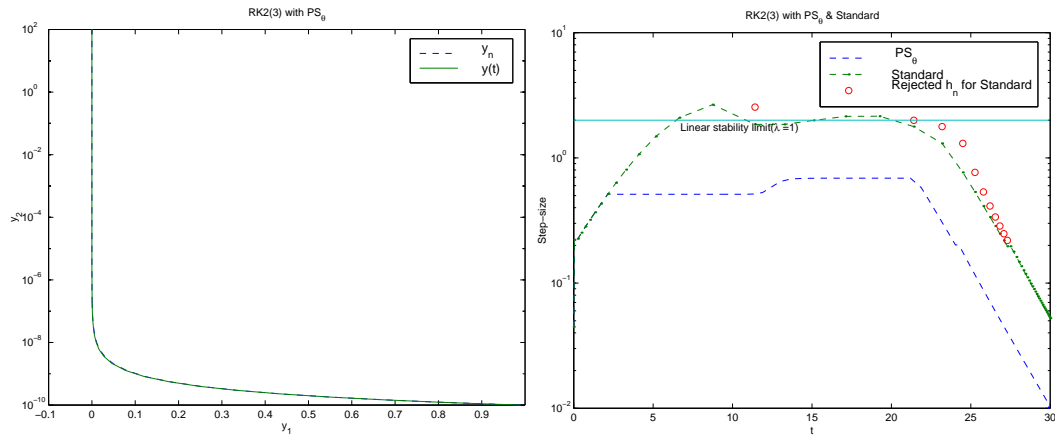
with the constant $c = 0$.

Fig. 4 (i) Numerical solution using RK2(3) with PS$_\theta$ augmented error control around a saddle point. (ii) Step-sizes used by the typical and PS$_\theta$ augmented algorithms.
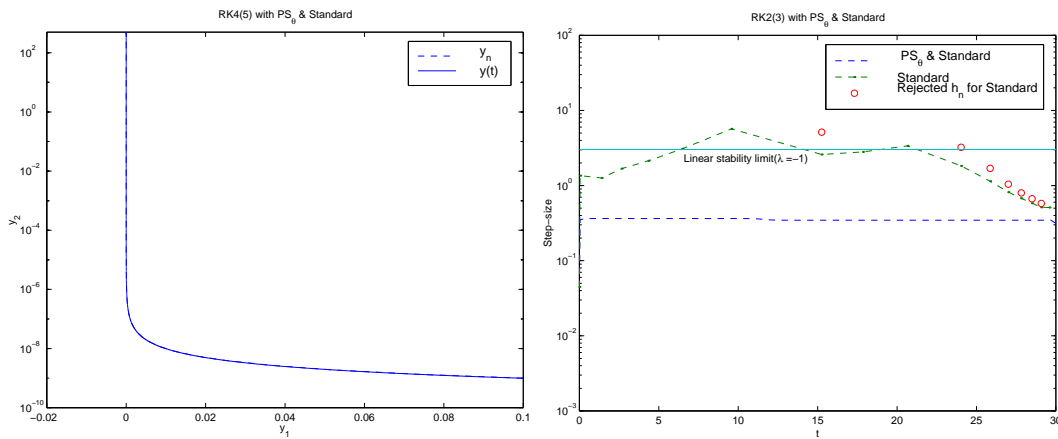

Fig. 5 (i) Numerical solution using RK4(5) with PS$_\theta$ augmented error control around a saddle point. (ii) Step-sizes used by the typical and PS$_\theta$ augmented algorithms.

The figures 6-8 show that PS$_\theta$ error control only determines step-sizes near fixed point and standard error control determines the step-sizes away from fixed points. In figure 9 we see that the PS$_\theta$ method controls the step-sizes in most of phase space since the value of φ reduces to 10^{-3}.
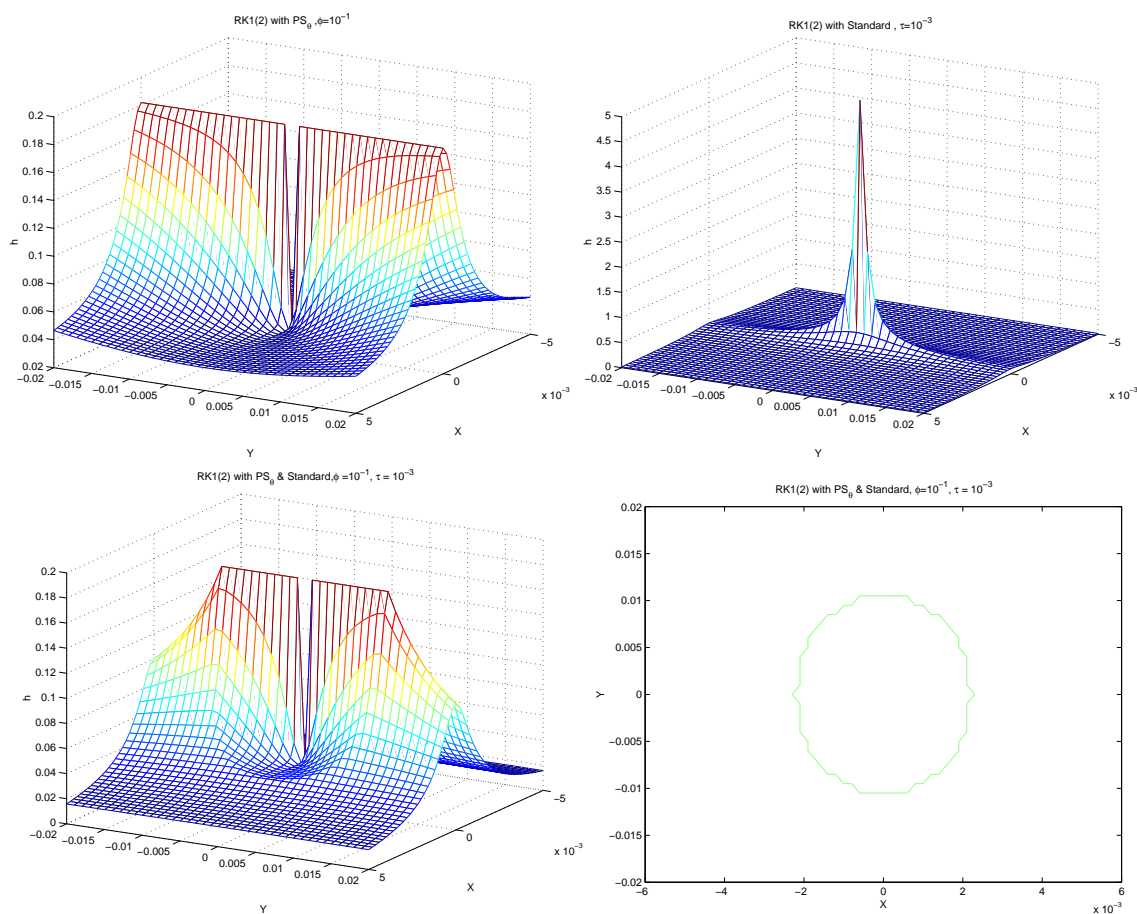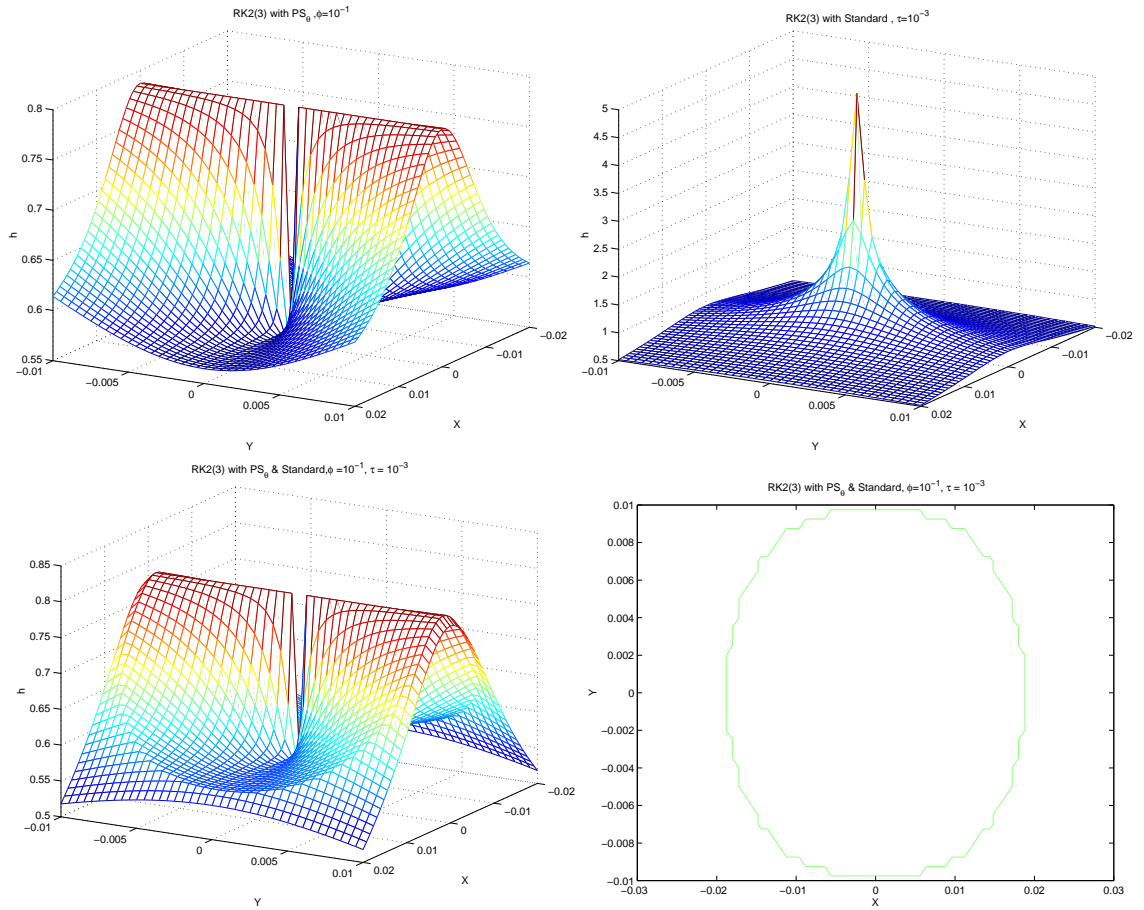
Fig. 6 Surface plot of the maximum acceptable step-size sequences when RK1(2) method is applied to the system (63) under (1) PS_θ error control. (ii) standard adaptive error control. (iii) PS_θ and standard (iv) PS_θ and standard, where the maximum step-sizes due to PS_θ is set at 1 and step-sizes due to standard is set at 0.
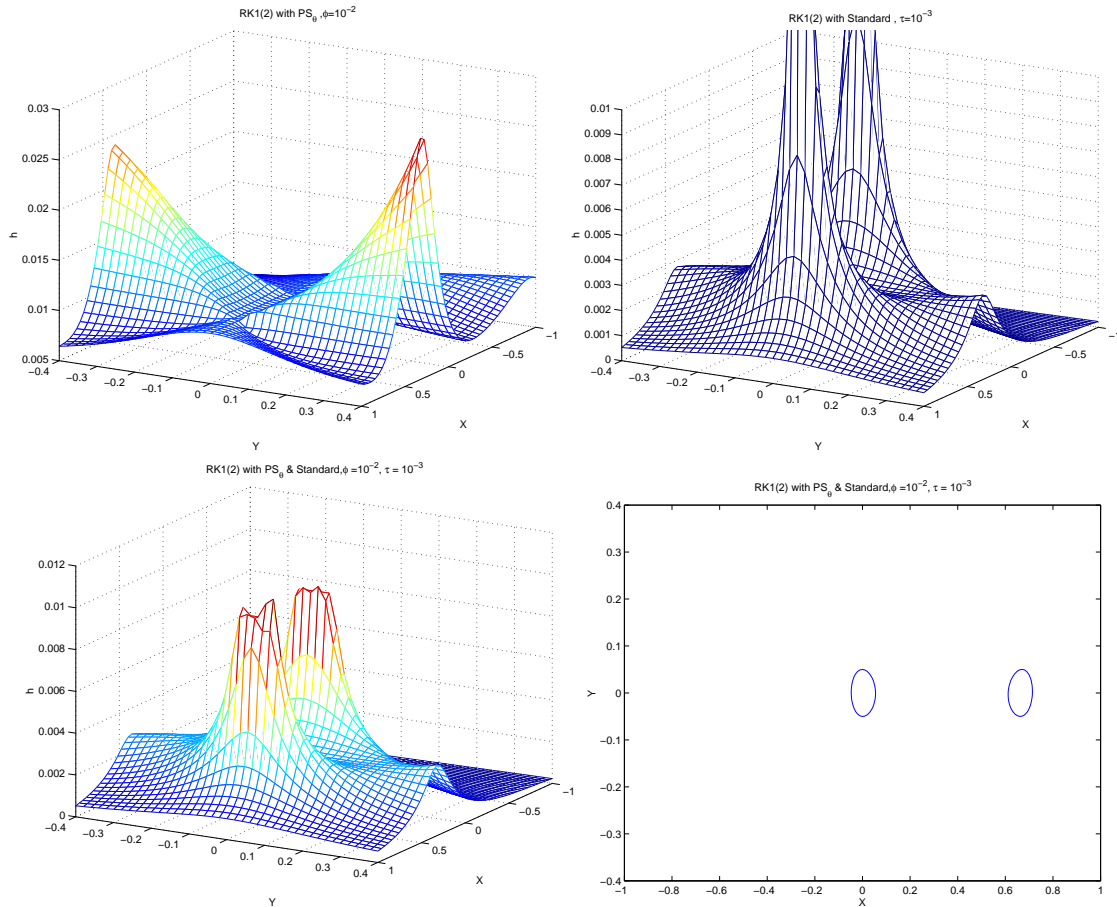
Fig. 7 Surface plot of the maximum acceptable step-size sequences when RK2(3) method is applied to the system (64) under (1) PS_θ error control. (ii) standard adaptive error control. (iii) PS_θ and standard . (iv) PS_θ and standard, where the maximum stepsizes due to PS_θ is set at 1 and step-sizes due to standard is set at 0.

Fig. 8 Surface plot of the maximum acceptable step-size sequences when RK1(2) method is applied to the system (65) under (1) PS_θ error control. (ii) standard adaptive error control. (iii) PS_θ and standard. (iv) PS_θ and standard ,where the maximum stepsizes due to PS_θ is set at 1 and step-sizes due to standard is set at 0.
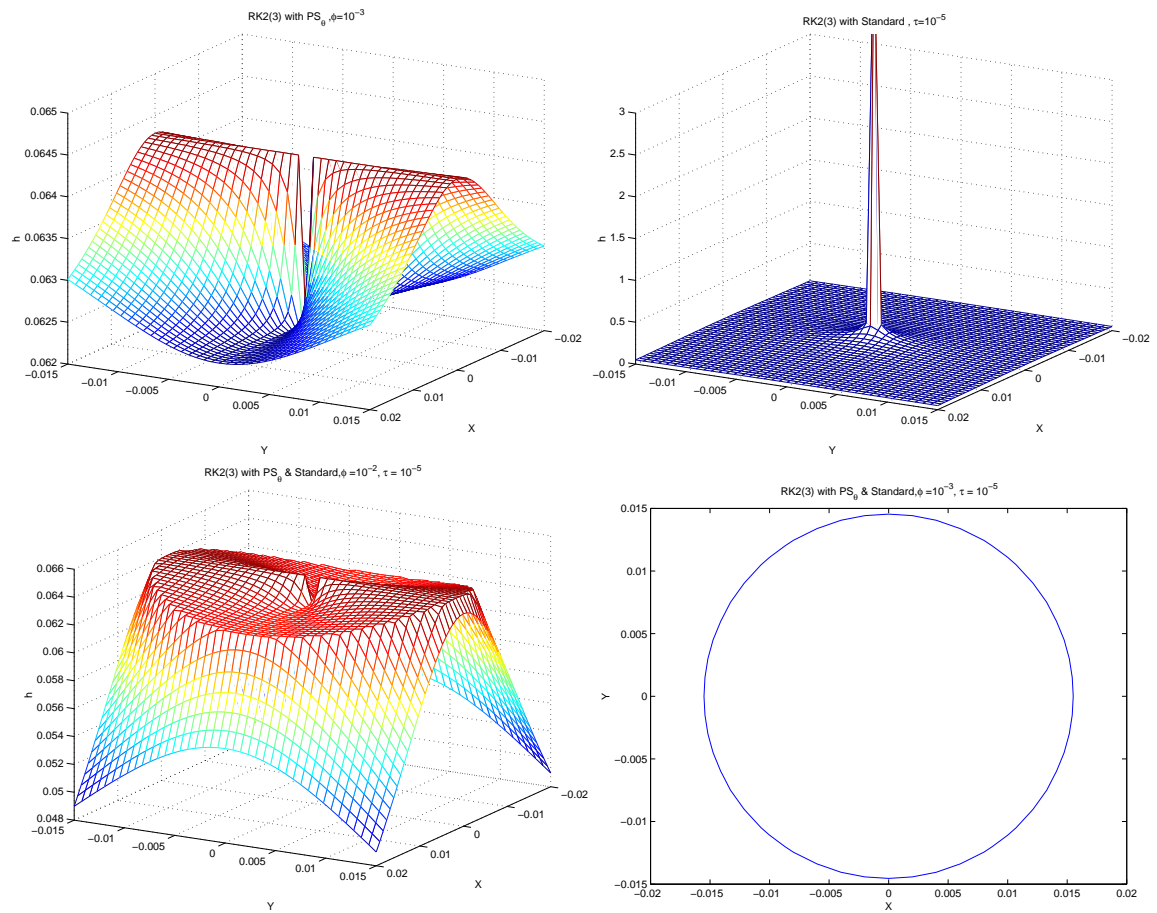
Fig. 9   Surface plot of the maximum acceptable step-size sequences when RK2(3) method is applied to the system (64) under PS$_\theta$ error control and standard adaptive error control with $\varphi = 10^{-3}$ and $\tau = 10^{-5}$.

4.4 Average step-size sequences

In this section, minimum, average and maximum step-sizes are computed for different values of φ when RK1(2) method with PS_θ constraint is applied to the scalar differential equation $y_t = -y$ and the linear system

$$y_t = \begin{bmatrix} -1 & 0 & 0 \\ 0 & -10 & 0 \\ 0 & 0 & -100 \end{bmatrix} y. \tag{66}$$

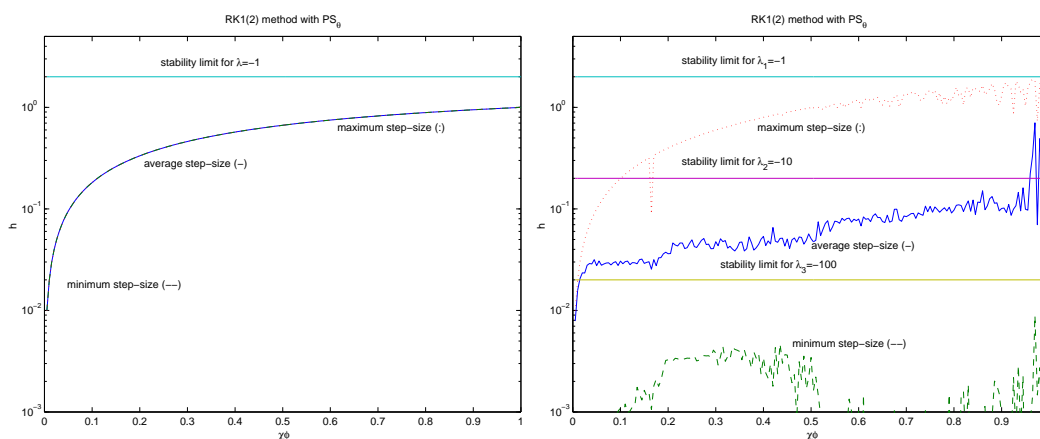These step-sizes are plotted against $\chi\varphi$

Fig. 10 (i) Minimum,average and maximum step-sizes when RK1(2) method is applied to the scalar equation $y_t = -y$ under PS_θ error control. (ii) Minimum, average and maximum step-sizes when RK1(2) method is applied to the system (66) under PS_θ error control .

The figure 10(i) shows that all steps are below the stability limit. This ensures the monotonic convergence of the solution. In figure 10(ii), we see that all steps are below the stability limit for $\lambda = -1$, ensuring the monotonic convergence of this component. It is also observed that the average step sizes are below the stability limit for $\lambda = -10$ except some step-sizes above this limit for $\chi\varphi > 0.9$ and average and maximum step-sizes are above the stability limit for $\lambda = -100$.

5 Conclusions

In summary, the error control (2) does not influence the numerical solution in most region of phase space, but improves the performance near fixed points. More precisely, the error control is designed to positively affect the linear stability property around true fixed points. The new step-size scheme, which is introduced in this paper, leads to stable step-sizes(with quadratics convergence, in the limit as $\varphi \to 0$, to a constant value) near fixed points.

In this paper, the PS_θerror control is analyzed only for forward Euler method applied to the linear system whose coefficient matrix has only real(negative) eigenvalues and it is shown that for the linear system of this type with a stable hyperbolic fixed point, the numerical solution which is forced to converge to the fixed point. The analysis of this error control for forward Euler method applied to the linear system, whose coefficient matrix has complex eigenvalues with negative real part, could be considered. The analysis of the error control for general explicit Runge-Kutta methods will also be possible. These two issues will be focused and analyzed in the forthcoming paper.

References

[1] M.A.Aves, D.F.Griffiths and D.J.Higham, *Does error control supress spuriosity?* SIAM J. NUm. Ana.,**34** :756 (1997).

[2] D.F.Griffiths, *The dynamics of some linear multistep methods.* In D.F.Griffiths and G.A.Watson, editors, Proceedings of the Dundee Conference on Numerical Analysis, 115–134 , Pitman Research Notes in Mathematics, 1988.

[3] E.Hairer, S.P.Nφrsett and G.Wanner, *Solving Ordinary Differential Equations I - Nonstiff Problems*, volume I, Springer-Verlag, Berlin Heidelberg, Second Edition, 1993.

[4] J.Hale and H.Kocak, *Dynamics & Bifurcations*, Springer - Verlag, New York Inc. 1991

[5] G.Hall, *Equilibrium states of Runge-Kutta Schemes I*, ACM Trans. on Math. Software, **11** : 289(1985).

[6] G.Hall, *Equilibrium states of Runge-Kutta Schemes II*, ACM Trans. on Math. Software, **12** : 183(1986).

[7] D.J.Higham and A.M.Stuart, *Analysis of the Dynamics of local error control via a piecewise continous residual*, BIT, **38** : 44 (1998).

[8] D.J.Higham, A.R.Humphries and R.J.Wain, *Phace space error control for Dyanamical Systems*, SIAM J. Sci. Comp., **21** : 2275(2000).

[9] A.R.Humphries and N.Christodoulou, *Phace space error control for Dyanamical Systems II* Research Report No: **2000-13**, Centre for Mathematical Analysis and Its Applications, Uni.of Sussex, UK.

[10] L.F.Shampine, *Numerical Solution of Ordinary Differential Equations*, Chapman and Hall, 1994.

[11] A.M.Stuart and A.R.Humphries, *The essential stability of local error control for Dyanamical Systems*, SIAM J. Num. Ana., **32** : 1940 (1995)

[12] A.M.Stuart and A.R.Humphries, *Dynamical Systems and Numerical Analysis*, Cambridge University Press, Cambridge, 1996.